THE AMERICAN SOCIETY OF MECHANICAL ENGINEERS
Three Park Avenue, New York, N.Y. 10016-5990

99-GT-3

A MECHANISM OF COMBUSTION INSTABILITY IN LEAN PREMIXED GAS TURBINE COMBUSTORS

Tim Lieuwen, Hector Torres, Clifford Johnson and Ben T. Zinn
Schools of Aerospace and Mechanical Engineering
Georgia Institute of Technology
Atlanta, GA 30332-0150

Abstract

There has been increased demand in recent years for gas turbines that operate in a lean, premixed (LP) mode of combustion in an effort to meet stringent emissions goals. Unfortunately, detrimental combustion instabilities are often excited within the combustor when it operates under lean conditions, degrading performance and reducing combustor life. To eliminate the onset of these instabilities and develop effective approaches for their control, the mechanisms responsible for their occurrence must be understood.

This paper describes the results of an investigation of the mechanisms responsible for these instabilities and approaches for their control. These studies found that combustors operating in a LP mode of combustion are highly sensitive to variations in the equivalence ratio (ϕ) of the mixture that enters the combustor. Furthermore, it was found that such ϕ variations can be induced by interactions of the pressure and flow oscillations with the reactant supply rates. The ϕ perturbations formed in the inlet duct (near the fuel injector) are convected by the mean flow to the combustor where they produce large amplitude heat release oscillations that drive combustor pressure oscillations. It is shown that the dominant characteristic time associated with this mechanism is the convective time from the point of formation of the reactive mixture at the fuel injector to the point where it is consumed at the flame. Instabilities occur when the ratio of this convective time and the period of the oscillations equals a specific constant, whose magnitude depends upon the combustor design. Significantly, these predictions are in good agreement with available experimental data, strongly suggesting that the proposed mechanism properly accounts for the essential physics of the problem. The predictions of this study also indicate, however, that simple design changes (i.e., passive control approaches) may not, in general, provide a viable means for controlling these instabilities, due to the multiple number of modes that may be excited by the combustion process. This conclusion indicates that active control strategies may be necessary for controlling these instabilities.

1. Introduction

Increasingly stringent emissions legislation has increased the demand for lean, premixed (LP) combustors (see Fig.1) that operate at low temperatures. However, LP systems are prone to detrimental combustion instabilities in various operating ranges, including the lean conditions where they are designed to operate [1]. To develop rational approaches for preventing or controlling these instabilities, an understanding of the controlling mechanism(s) and capabilities for predicting the conditions under which they occur must be developed. Intensive experimental and theoretical work has been performed during the past few years [1-17] to understand these mechanisms and to develop effective approaches for their control. A number of experimental studies have characterized the operating conditions under which LP combustion instabilities occur [1-7]. Also, several theoretical studies have attempted to elucidate the mechanism(s) that drive the instability and to develop models that can predict their occurrence [8-13]. Yet, in spite of these efforts, there is no consensus about the mechanisms that are responsible for the onset and sustenance of these instabilities.

Presented at the International Gas Turbine & Aeroengine Congress & Exhibition
Indianapolis, Indiana — June 7-June 10, 1999

Prior theoretical studies by the authors suggested that heat release oscillations excited by fluctuations in the composition of the reactive mixture entering the combustion zone were the dominant mechanism responsible for the instabilities observed in these combustors [10-12]. However, limited experimental evidence was available to critically assess the theory. Furthermore, the developed theory could not account for the observed dependence of the combustor stability upon flame structure. This paper describes recent work of the authors that extends the theory to account for flame structure effects, as well as comparisons of the theory with measurements at several facilities.

The following section presents the mechanism of instability proposed by the authors, necessary conditions under which it will cause self-excited oscillations, and an analysis that can be used to predict the conditions under which combustors become unstable. Next, it presents results that illustrate the agreement between the predictions of the developed theory and experimental data. The paper closes with a discussion of possible approaches for passive control and of other potential instability mechanisms.

2. Mechanism of LP Combustion Instability

The primary difficulty in combustion instability studies is understanding the interactions between the unsteady heat release processes and the disturbances that drive them. This task is difficult because these heat release oscillations may be due to oscillations of the velocity, pressure, temperature, and reactants composition that are present simultaneously in combustion systems. Though heat release oscillations may be excited by a host of disturbances, there are two conditions which must be met for self-excited, combustion driven oscillations to occur. First, the unsteady heat release processes must be in phase with the fluctuating acoustic pressure so that energy is added to the unsteady motions (i.e., Rayleigh's criterion) [10]. Second, the rate of energy addition must exceed the rate of energy dissipation.

This section describes a mechanism that appears to be responsible for LP combustion instabilities, shows what operating ranges will satisfy the conditions discussed above, and consequently, predicts the regions under which instabilities will be observed. A schematic of the feedback process upon which the proposed mechanism is based on is shown in Fig. 2. Its main elements are the generation of heat release oscillations by periodic variations in ϕ of the reactive mixture that enters the flame, and the formation of ϕ oscillations in the inlet section by velocity and pressure oscillations in the vicinity of the fuel injector. These processes are described in more detail in the following subsections.

2.1 Response of LP systems to ϕ oscillations

This study was partially motivated by observations that properties of premixed combustion systems, such as flame thickness, flame speed, and reaction rate become increasingly sensitive to variations in ϕ as the combustion process stoichiometry becomes leaner [10]. Moreover, systems operating near the lean limit are acutely sensitive to ϕ perturbations since they may cause periodic extinction of the combustion process. To further examine these observations, an unsteady well stirred reactor (WSR) model was developed and its response to ϕ perturbations in its inlet conditions was studied [10]. Figure 3 presents a result from this study. It shows that the response of the WSR's reaction rate to perturbations in the inlet ϕ significantly increases (by two orders of magnitude) as the mean value of ϕ decreases. This result strongly suggests that ϕ oscillations could drive substantial heat release oscillations under lean operating conditions. It also suggests that ϕ oscillations are unlikely to drive instabilities near stoichiometric conditions because of the negligible response of the reaction rate at this operating condition. Some experimental observations that the oscillating pressure amplitude in LP combustors is relatively small under stoichiometric conditions and becomes progressively larger as ϕ is reduced [1] appear to support these assertions and the trends depicted in Fig. 3.

2.2 Formation of ϕ oscillations

The discussion in Section 2.1 suggests that the sensitivity of LP systems to ϕ oscillations could be responsible for their unstable behavior. While random ϕ fluctuations undoubtedly occur in LP combustors (e.g., due to turbulent mixing), ϕ fluctuations can only play a role in an instability mechanism if they are driven by the combustion process and the resulting pressure and velocity oscillations, thus closing the feedback loop needed to maintain an instability, see Fig. 2. Consequently, it is necessary to consider how ϕ fluctuations can arise, and to elucidate the feedback mechanism between the ϕ and heat release oscillations that drive the instability. The following equation, derived from the definition of ϕ, suggests a mechanism for the formation of ϕ oscillations in the inlet section due to velocity and pressure perturbations:

$$\frac{\phi'}{\phi} = \frac{\dfrac{\dot{m}'_f}{\dot{m}_f} - \dfrac{\dot{m}'_o}{\dot{m}_o}}{1 + \dfrac{\dot{m}'_o}{\dot{m}_o}} \qquad (1)$$

In Eq. (1), the subscripts f and o denote fuel and oxidizer (assumed to be air from this point on), respectively, and m the mass flow rate. This equation shows that ϕ oscillations can be formed by air and/or fuel flow oscillations (that are present at the fuel injector). Furthermore, for the low Mach number flows typical of these systems, this equation implies that small acoustic fluctuations can generate significant ϕ fluctuations; e.g., for M= 0.05 and a choked fuel injector (i.e., $m_f'=0$),

acoustic oscillations of 1% of the mean (i.e., $u'/\bar{c} = 0.01$) will generate ϕ oscillations of 20% (i.e., $\phi'/\bar{\phi}=0.20$, because $\frac{\phi'}{\bar{\phi}} \approx \frac{1}{M}\frac{u'}{c}$). The possibility of forming such large amplitude ϕ oscillations from modest flow perturbations suggests that even though diffusive and turbulent mixing processes will tend to homogenize the mixture as it flows from the fuel injector towards the combustor, the ϕ fluctuations may still persist at the flame.

This discussion suggests that acoustic oscillations in a combustion chamber similar to the one shown in Fig. 1 may be accompanied by oscillations in the composition of the reactive mixture in the inlet section. Furthermore, Fig. 2 shows that the presence of these ϕ oscillations in the inlet section are a critical component of this mechanism of instability. It is significant that measurements of such oscillations have been recently reported by Mongia *et al.* [14]. This paper presented measurements of fuel mass fraction oscillations in the combustor inlet section with frequencies corresponding to the instability frequency, confirming the presence of oscillations in the reactive mixture composition predicted in this section.

2.3 Conditions for Instability

The discussions in Sections 2.1 and 2.2 have outlined the framework for a combustion instability mechanism that is potentially responsible for those observed in LP combustors. This mechanism and its controlling steps/parameters can be better understood by considering the time evolution of the various processes that sustain it, see Fig. 4 (see Ref. [18] for the application of similar methods of analysis to other combustion systems). Figure 4-a shows the time dependence of the acoustic pressure at the flame of an unstable mode with a period T (the length of the combustion region is assumed to be very small relative to a wavelength). This disturbance propagates upstream into the inlet duct and produces pressure oscillations at the fuel injector, see Fig. 1. As long as no pressure node exists between the flame and fuel injector (implying a one hundred eighty degree phase change across the node) and the Mach number is low, the pressure disturbance at the flame and fuel injector will be nearly in phase, see Fig. 4-b.

These pressure oscillations will be accompanied by fluctuations in the velocity, and therefore the oxidizer flow rate at the fuel injector. However, the phase of these velocity oscillations relative to the pressure will depend on the upstream boundary conditions (e.g., if the upstream boundary is a pressure node, the velocity will lead the pressure by ninety degrees). For the sake of brevity, we will carry out this analysis assuming a pressure node boundary condition and quote the results for the other cases.

For low Mach number flows, the velocity and mass flow rate will be nearly in phase, see Fig. 4-c. Assuming choked fuel flow (i.e., $m_f'=0$), Eq. (1) shows that the fluctuating ϕ of the reactive mixture formed in the vicinity of the fuel injector will be out of phase with these air flow oscillations, see Fig. 4-d. This leads to the formation of a reactive mixture with a periodically varying ϕ that is convected by the flow and reaches the base of the flame after a convective time, $\tau_{convect}$, see Fig. 4-e.

The reactive mixture will not be consumed instantly when it reaches the flame base (even when any delays due to purely chemical kinetic processes are neglected) because "different parts" of the flow entering the combustor will be consumed at different locations of the flame surface and the mixture will not be completely consumed until it reaches the end of the flame region, see Fig. 1. Thus, the total (i.e., spatially integrated) heat release will lag the ϕ oscillation at the base of the flame by a time, τ_{eq} (to be discussed later), see Fig. 4-f. It follows from Rayleigh's criterion that an instability can occur if the heat release oscillations in Fig. 4-f are in phase with the pressure oscillations at the flame in Fig. 4-a; that is, if:

$$\textbf{Pressure node: } \frac{\tau_{convect} + \tau_{eq}}{T} = C_n = n - 1/4 \quad n=1, 2... \quad (2)$$

Using a similar analysis, it can be shown that if the upstream inlet boundary is an acoustically rigid or nonreflecting surface, the corresponding conditions for instability become [11]:

$$\textbf{Velocity node: } \frac{\tau_{convect} + \tau_{eq}}{T} = C_n = n - 3/4 \quad (3)$$

$$\textbf{Nonreflecting: } \frac{\tau_{convect} + \tau_{eq}}{T} = C_n = n \quad (4)$$

Finally, for situations where the fuel injector is unchoked and the dominant contribution to the ϕ fluctuation comes from fuel flow modulation, see Eq. (1), the instability condition is [11]:

$$\textbf{Fuel Flow Modulation: } \frac{\tau_{convect} + \tau_{eq}}{T} = C_n = n - 1/2 \quad (5)$$

Thus, instability regions are primarily a function of $(\tau_{convect} + \tau_{eq})/T$, which will be denoted as $\tau_{conv,eff}/T$. Specifically, Eqs. (2-5) indicate that the regions of instability approximately center about locations where $\tau_{conv,eff}/T = C_n$, where C_n is a constant that depends on the combustor configuration. In a combustion system without damping, these instability regions will lay in bands where $C_n - 1/4 < \tau_{conv,eff}/T < C_n + 1/4$ (that is, the limits occur where the phase between the acoustic pressure and heat release is ninety degrees). Figure 5 illustrates the instability regions for the combustor configurations considered above.

Note that it is possible that a region where instability can occur will actually remain stable if the energy addition due to the unsteady heat release can not overcome damping processes. For example, the negligible response of the reaction rate to ϕ fluctuations under stoichiometric conditions, see Fig. 3,

suggests that even when the operating conditions are conducive to an instability, see Fig. 5, the combustor will remain stable (or else become unstable due to some other mechanism). For operating conditions where unstable combustion occurs, the presence of damping will narrow the "width" of the instability regions, causing the "edges" of otherwise unstable regions to become stable.

2.4 Stability Calculations

In order to use these results to predict conditions for instability in real systems, the quantity $\tau_{conv,eff}/T$, and thus the convective times, $\tau_{convect}$ and τ_{eq}, must be determined. The convective time, $\tau_{convect}$, can be approximated as the distance from the fuel injector to the base of the flame, divided by the average flow velocity in the inlet, see Fig. 1:

$$\tau_{convect} = L_{inj} / \bar{u} \tag{6}$$

More sophisticated computations that better characterize the multidimensional flow dynamics in the inlet section (in order to better understand the convective processes in the inlet section) have been reported in [9]. However, the results of this study seem to indicate that Eq. (6) is a good approximation, although additional effects, such as stratification of ϕ in the radial direction, were noted.

Determining τ_{eq} is more difficult. Since different parts of a given cross section of reactive mixture are consumed at different times and places, the effects of the structure of the flame region and the phasing of the ϕ fluctuation when it is consumed are important, see Fig. 1. Although these effects have previously been noted by the authors [11] and by Straub and Richards [3], no attempts were made to quantify them. An analysis that accounts for these effects in a slightly different context has been previously presented by Putnam [18] however.

A more general analysis than that given in Ref. [18] to determine this characteristic time is given in the Appendix. The analysis is general enough to account for three dimensional non-uniformities in the reactive mixture composition and a complex flowfield and flame structure. Thus, it can be used in conjunction with computational results of the mean properties of the combustor to predict its stability behavior.

A convenient relation between $\tau_{conv,eff}$ and $\tau_{convect}$ can be derived by defining a "flame length correction coefficient", α (see Appendix):

$$\frac{\tau_{conv,eff}}{T} = \frac{\tau_{convect}}{T}\left(1+\alpha\frac{L_{flame}}{L_{convect}}\right) \tag{7}$$

The coefficient α is a function of the flame Strouhal number, $St=fL_{flame}/u$, and the structure of the flame region. Physically, α represents the fractional location of a hypothetical flame sheet that consumes the entire mixture at one point downstream of the flame base. For example, a value of $\alpha = 1/3$ implies that the phase introduced between the ϕ oscillation at the base of the flame and the heat release from the distributed flame region is equivalent to that from a hypothetical flame sheet located at $L_{flame}/3$.

Figure 6 shows the results of several calculations of α, illustrating its behavior for different flame shapes over a range of Strouhal numbers (α is given by Eq. (A-16) in the Appendix). An examination of Fig. 6 reveals several noteworthy characteristics of α. First, note that at low Strouhal numbers, α is only a function of the flame shape and independent of the Strouhal number. Second, the figure illustrates the sensitivity of α to the Strouhal number when St~O(1). For example, note that for the curved flame, a change in the value of the Strouhal number of less than five percent results in a change of α by sixty percent when St=1.4. To obtain a feel for ranges these values may take in typical combustors, if it is assumed that f=200 Hz, L_{flame}=2 – 5 cm, $L_{convect}$=5 – 10 cm, and $\bar{u}$=30 - 60 m/s, then St ~ 0.05 – 0.4, implying that α ~ 0.5 (see Fig. 6). Thus, Eq. (7) shows that $\tau_{conv,eff} \sim (1 - 1.5)\tau_{convect}$.

3. Comparisons with Experimental Results

The theory developed in the prior section shows that combustion instabilities induced by ϕ oscillations will occur under conditions where the value of $\tau_{conv,eff}/T$ is within certain ranges, see Fig. 5. It follows that combustor data should correlate with this parameter when ϕ oscillations are responsible for the instabilities. However, as the analysis and results in the prior section show, it may be difficult to determine $\tau_{conv,eff}/T$ because of its dependence on the length and structure of the flame region. Since the value of $\tau_{convect}$ in a given experimental configuration is much easier to determine, the theory developed in this paper suggests that unstable combustor situations occur when:

$$\frac{\tau_{convect}}{T} = \frac{C_n}{\left(1+\alpha\frac{L_{flame}}{L_{convect}}\right)} = \tilde{C}_n(St, f(\xi)) \tag{8}$$

The estimates of typical values in the previous section suggest that instabilities will occur where $\tau_{convect}/T \sim (0.7\text{-}1)C_n = \tilde{C}_n$. Note that since $\tilde{C}_n \le C_n$, measured instability regions plotted versus $\tau_{convect}/T$ will always lie to the left of those predicted in Fig. 5 or in Eqs. (2-5).

The rest of this section presents experimental results from several facilities showing that the regions of instability are primarily a function of $\tau_{convect}/T$, in agreement with the predictions of this paper. These results also show that the

measured dependence of the instability regions on the upstream boundary condition in Fig. 5 are well described by the theory.

Figure 7 shows pressure data obtained by Straub and Richards [3] and the instability regions predicted by Eq. (2). It can be seen that their data collapses into bands when normalized by $\tau_{convect}/T$, as predicted in the preceding discussion. Furthermore, since the inlet section of the combustor was connected to a plenum (see [3]), the upstream boundary condition may be approximated as a pressure node. Then, Eq. (2) predicts that instabilities should occur in the vicinity of $\tau_{convect}/T = 0.75, 1.75, \ldots$. The figure shows that this prediction is in agreement with the measured data, particularly for the first region of instability. It can be seen that the agreement is not as good for the second band of oscillations; however, this is likely due to distributed flame effects and is discussed further below.

Figure 8 shows unsteady pressure data obtained at Penn State [2,19]. Since the upstream boundary of the inlet section in this facility is essentially nonreflecting, Eq. (4) predicts that instabilities should occur when $\tau_{convect}/T = 0, 1, \ldots$. Figure 8 shows that the measured data agrees well with this prediction.

Figure 9 shows unsteady pressure data obtained at Georgia Tech (a description of the experimental setup and additional results can be found in [17]). Since the upstream boundary of the inlet section is rigid, Eq. (3) predicts that instabilities should occur when $\tau_{convect}/T = 0.25, 1.25, \ldots$. Figure 9 shows that most of the large amplitude pressure oscillations occur in the predicted region. However, it should be noted that instabilities were observed in four test runs that are well outside of the predicted unstable region (i.e., $\tau_{convect}/T=0.65$).

An examination of Figs. 7-9 reveals that some of the measured instabilities occurred in $\tau_{convect}/T$ regions that lie to the left of the predicted regions. As the discussion below Eq. (8) indicates, this consistent leftward bias is to be expected, however, because regions of instability should actually occur where $\tau_{convect}/T \sim (0.7\text{-}1)C_n = \tilde{C}_n$; i.e., between zero and thirty percent to the left of those shown in Fig. 5. The shift of approximately twenty five percent in the DOE data (see Fig. 7) and twenty percent in the Georgia Tech data (see Fig. 9) suggests that these "discrepancies" are simply due to correlating the measure data with $\tau_{convect}/T$ instead of $\tau_{conv,eff}/T$.

The above comparisons between the theoretical predictions and the experimental data clearly demonstrate that LP instabilities occur at specific ranges of the parameter $\tau_{convect}/T$. Significantly, the demonstrated agreement between the theory's predictions and measurements strongly suggests that the mechanism discussed in this paper is responsible for LP instabilities.

One issue that is not clear, however, is the lack of unstable oscillations in bands that are predicted to be unstable. For example, no oscillations have been observed in the Georgia Tech facility in the $0<\tau_{convect}/T<0.5$ band even though the combustor has been run under operating conditions where the frequency of some of its natural modes would lie in this unstable range. Excitation of other modes that correspond to higher instability bands, such as $2<\tau_{convect}/T<2.5$, have been observed, however, but the dominant unstable mode still corresponds to $1<\tau_{convect}/T<1.5$.

4. Passive Control Considerations

An understanding of the mechanisms responsible for LP instabilities may provide combustor designers with means for eliminating these instabilities in the design stage. For example, one gas turbine manufacturer (Solar Turbines) has eliminated instabilities by designing a combustor whose operating regions lie outside of the unstable range. Specifically, Solar has modified $\tau_{convect}$ by changing the combustor inlet diameter and fuel injector location [20].

In spite of Solar's success, shifting the value of $\tau_{conv,eff}/T$ outside the unstable range may be difficult to achieve in practice because of design restrictions. Also, several different combustor modes may be excited, and stabilizing one of these modes may destabilize another. For example, Fig. 10 presents data obtained at the Georgia Tech facility, illustrating the dependence of the unsteady pressure amplitude upon the velocity in the inlet section. It shows that at lower velocities, the 430 Hz mode is excited, and that its amplitude decreases with increasing velocity. However, as the inlet velocity is further increased, the 630 Hz mode becomes unstable because its period, T, is smaller, and the parameter $\tau_{conv,eff}/T$ is within the unstable range. Figure 10 shows that the combustor is "quiet" only within a narrow velocity range.

Similar observations have been made by Straub and Richards [3] who moved the location of the fuel injector and found that stabilizing one mode was often accompanied by destabilization of another (they show that these problems may be dealt with by injecting the fuel at multiple locations). These examples illustrate the potential shortcomings of passive control approaches.

5. Final Remarks

This paper has shown that LP combustion instabilities are likely due to a feedback process between the heat release, acoustic pressure, and ϕ oscillations, see Fig. 2. Furthermore, it has been shown that regions of instability primarily depend upon the parameter $\tau_{convect}/T$, implying that the frequency of oscillation, the mean velocity, and the location of the fuel injector are key parameters affecting combustor stability.

In closing, we would like to reiterate that while this paper has demonstrated that combustion instabilities in LP systems are likely due to ϕ oscillations, it is possible that other mechanisms may also be important. Thus, it should be noted that some studies have concluded that other mechanisms, such as combustion within coherent vortical structures [4, 5], are responsible for instabilities in these systems. These

conclusions appear to be based on observations of such structures during unstable combustion [4, 5].

While it is altogether possible that other mechanisms for instability (such as combustion in vortices) are important, care must be exercised in assessing a mechanism of instability based on observations of unstable combustion at the limit cycle; that is, it is possible that some instability mechanism causes growth of the amplitude of the unsteady motions in a combustor, eventually forcing the periodic shedding of these structures. Thus the presence of these structures does not necessarily supply any information about the *origin* or *mechanism* that initiated the instability. In the same manner, the measurements of ϕ oscillations by Mongia *et al.* [14] during unstable combustion cannot be interpreted as an indication that ϕ oscillations are responsible for initiating the instability. While Eq. (1) shows that such ϕ oscillations can be excited by acoustic oscillations in the inlet, the instability mechanism that is responsible for exciting these oscillations could be due to a totally different mechanism (e.g., vortex shedding).

This discussion shows that observations of combustion instabilities at the limit cycle may not provide useful information about the origin of the instability. Consequently, any conclusions regarding the instability should be based on an analysis of the conditions necessary for such a mechanism to be self-exciting, and determining whether instability data can be correlated with such a condition. The demonstrated agreement between our predictions and the data measured in a number of facilities strongly suggest that this mechanism is related to ϕ oscillations.

6. Appendix

This appendix presents a derivation of an expression for the characteristic time, τ_{eq} that generalizes a previous analysis of Putnam [18]. It extends the definition of the convective time to account for the fact that the combustible mixture is consumed over a finite flame region (rather than at a single point). Denoting the flame's instantaneous rate of heat release per unit area by $q'(x_f,t)$, the total rate of heat release within the flame, $Q'(t)$, is given by:

$$Q'(t) = \iint_{\substack{\text{Flame}\\ \text{Surface}}} q'(x_f,t)\,dx_f \qquad \text{(A-1)}$$

where x_f is the mean flame location. Note that in writing Eq. (A-1), it is assumed that the heat release occurs along a flame surface. However, this development can be readily generalized to a region of distributed heat release as well.

Since this study is interested in heat release fluctuations induced by mixture composition oscillations, Eq. (A-1) is written as:

$$Q'(t) = \iint_{\substack{\text{Flame}\\ \text{Surface}}} K(\phi(x_f),x_f,t)\phi'(x_f,t)\,dx_f \qquad \text{(A-2)}$$

where K is a transfer function relating the instantaneous, local fluctuating rate of heat release to the fluctuating ϕ'. If the rate of heat release is only a function of the local ϕ', then K is a constant. However, the local heat release may be a function of the heat release at other parts of the flame due to flame dynamics effects. In this case, K is a function of space, time, and the instantaneous ϕ' at other parts of the flame. These cases will be referred to as "locally" and "globally" reacting, respectively.

Neglecting molecular transport and chemical reaction, the ϕ' of the mixture entering the flame at x_f, can be related to ϕ' at the base of the flame at x_b (see Fig. 1) by the following species transport equations for the fuel and oxidizer mass fractions:

$$\frac{\partial Y_F}{\partial t} + u\cdot\nabla Y_F = 0 \qquad \text{(A-3)}$$

$$\frac{\partial Y_{Ox}}{\partial t} + u\cdot\nabla Y_{Ox} = 0 \qquad \text{(A-4)}$$

Defining a constant k_ϕ by the relation $k_\phi Y_f/Y_{ox}=\phi$, multiplying Eq. (A-3) by k_ϕ/Y_{ox}, Eq. (A-4) by $-k_\phi Y_f/Y_{Ox}^2$ and adding the resulting equations yields the following equation for the evolution of ϕ:

$$\frac{\partial \phi}{\partial t} + u\cdot\nabla\phi = 0 \qquad \text{(A-5)}$$

Equation (A-5) shows that ϕ is constant along a pathline. Consequently, ϕ at the base of the flame, x_b, can be related to ϕ at the flame surface, x_f, by the expression:

$$\phi(x_f(u,x_b,t_b),t) = \phi(x_b,t_b) \qquad \text{(A-6)}$$

The equation of the pathline relating x_f at time t to x_b at time t_b is:

$$\frac{dx_\ell}{dt} = u(x_\ell,t) \qquad \text{(A-7)}$$

Generally, Eqs. (A-6) through (A-7) could be used to relate ϕ_f to ϕ_b using, for example, computed or measured descriptions of the mean flow fields and mixture composition. We will now simplify these equations in order to demonstrate their application, and to gain insight into the processes that affect τ_{eq}. The following assumptions are made: 1) the flowfield is uniform, one dimensional, and axisymmetric, 2) ϕ variations are one dimensional, and 3) the flame responds only to local ϕ disturbances (i.e., it is "locally" reacting).

It should be noted that the third assumption essentially treats the flame surface as a continuous distribution of reactors that do not interact with each other. Although these interactions likely occur in reality, we are not aware of any theory that can account for them. An attempt has been made in a slightly different context to model the flame as a dynamic surface that would account for these interactions; however, this analysis assumed a laminar flame [21]. Since it is not clear how closely, if at all, the dynamics of a turbulent flame conform to those of a laminar one, we have not pursued this approach.

Using assumptions 1-3, Eq. (A-2) can be simplified to:

$$Q'(t) = \int_{\text{Flame}} K\phi'(x_f, t)(2\pi y_f)dy_f \qquad \text{(A-8)}$$

Considering only the fluctuating component of ϕ and using assumptions 1 and 2, Eq. (A-5) and (A-6) can be written as:

$$\phi'(x_f, t) = \phi'(t - t_b - \frac{x_f - x_b}{u}) \qquad \text{(A-9)}$$

Assuming harmonic oscillations (i.e., $\phi'(x,t) = \phi'(x)e^{-i\omega t}$), defining a flame Strouhal number, $St=fL_{flame}/u$, and defining an equation of the flame surface, $(x_f-x_b)/L_{flame}=f(y/r)=f(\xi)$, Eqs. (A-8) and (A-9) can be combined to yield the following expression:

$$Q'(t) = 2\pi r^2 K\phi'(x_b, t_b)e^{-i\omega(t-t_b)} \int_{\substack{\text{Flame}\\ \text{Surface}}} \xi e^{2\pi i St f(\xi)}d\xi \qquad \text{(A-10)}$$

Finally, defining the quantity $Q_o(t)$ as the fluctuating heat release that would have occurred if all the reactive mixture was burned at the base of the flame, Eq. (A-10) can be written as:

$$Q'(t)/Q_O(t) = 2 \int_{\substack{\text{Flame}\\ \text{Surface}}} \xi e^{2\pi i St f(\xi)}d\xi = \kappa e^{i\omega\tau_{eq}} \qquad \text{(A-11)}$$

where $\kappa = |Q'(t)/Q_o(t)|$ and τ_{eq} is an "equivalent" time delay that accounts for the fact that different fractions of the combustible mixture that enters the combustor are burned at different instances. It follows from Eq. (11) that:

$$\omega\tau_{eq} = \tan^{-1}\left[\frac{\int_{\substack{\text{Flame}\\ \text{Surface}}} \xi \sin(2\pi St f(\xi))d\xi}{\int_{\substack{\text{Flame}\\ \text{Surface}}} \xi \cos(2\pi St f(\xi))d\xi}\right] \qquad \text{(A-12)}$$

$$\kappa = 2\left[\left[\int_{\substack{\text{Flame}\\ \text{Surface}}} \xi \sin(2\pi St f(\xi))d\xi\right]^2 + \left[\int_{\substack{\text{Flame}\\ \text{Surface}}} \xi \cos(2\pi St f(\xi))d\xi\right]^2\right]^{1/2} \qquad \text{(A-13)}$$

Equations (A-12) and (A-13) can be used to determine the quantities τ_{eq} and κ for a specified flame surface, $f(\xi)$. For example, if all the fuel burns in a planar flame at $x=x_b$, then the surface is described by $(x_f-x_b)/L_{flame}=f(\xi)=0$, yielding:

$$Q'(t)/Q_O = 2\int_0^1 \xi e^{2\pi i St*0}d\xi = 2\int_0^1 \xi d\xi = 1 \Rightarrow \qquad \kappa = 1, \tau_{eq} = 0 \qquad \text{(A-14)}$$

as expected.

Finally Eq. (A-11) suggests that the effect of having the heat released along the flame is equivalent to having the energy released at some "effective" flame location. Defining an "equivalent" nondimensional flame location $\alpha=L_{eq}/L_{flame}$, then the left side of Eq. (A-12) can be rewritten as follows:

$$\omega\tau_{eq} = 2\pi f\frac{L_{eq}}{u} = 2\pi\frac{fL_{flame}}{u}\frac{L_{eq}}{L_{flame}} = 2\pi St\alpha \qquad \text{(A-15)}$$

Combining Eqs. (A-12) and (A-15) yields:

$$\alpha(St, f(\xi)) = \frac{1}{2\pi St}\tan^{-1}\left[\frac{\int_{\substack{\text{Flame}\\ \text{Surface}}} \xi \sin(2\pi St f(\xi))d\xi}{\int_{\substack{\text{Flame}\\ \text{Surface}}} \xi \cos(2\pi St f(\xi))d\xi}\right] \qquad \text{(A-16)}$$

In the limit when $St<<1$, Eq. (A-16) simplifies to:

$$\alpha(f(\xi)) = \frac{\int_{\text{Flame Surface}} \xi f(\xi) d\xi}{\int_{\text{Flame Surface}} \xi \, d\xi} \qquad \text{(A-17)}$$

showing that in this case α is independent of the flame Strouhal number. The nondimensional effective convective time can be then defined as:

$$\frac{\tau_{conv,eff}}{T} = \frac{\tau_{convect}}{T}\left(1 + \alpha \frac{L_{flame}}{L_{convect}}\right) \qquad \text{(A-18)}$$

Figure (6) presents results of calculations that describe the dependence of α upon St and $f(\xi)$. These results are discussed in the Stability Calculations section.

7. Acknowledgments

This research was supported by AGTSR under Contract No. 95-01-SR031; Dr. Daniel B. Fant, Contract Monitor.

8. References

1.) Cohen, Jeffrey, Anderson, Torger, AIAA paper # 96-0819 (1996).

2.) Broda, J.C., Seo, S., Santoro, R.J., Shirhattikar, G., Yang, V., *Twenty Seventh Symposium (International) on Combustion*, The Combustion Institute, Pittsburgh, PA, (1998).

3.) Straub, D.L., Richards, G.A. ASME paper # 98-GT-492, (1998).

4.) Paschereit, C., Gutmark, E., Weisenstein, W., *Twenty Seventh Symposium (International) on Combustion*, The Combustion Institute, Pittsburgh, PA, (1998).

5.) Venkataraman, K.K, Simons, D.W., Preston, L.H., Lee, J., Santavicca, D.A. *Proceedings of the Eastern States Meeting of the Combustion Institute*, pp. 313-316, 1997.

6.) Anderson, Torger, Morford, Stephen, ASME paper #98-GT-568.

7.) Janus, M.C., Richards, G.A., Yip, M.J., ASME paper #97-GT-266.

8.) Janus, M.C., Richards, G.A., *Proc. Of the 1996 AFRC Intl. Symp.*, Baltimore, MD, 1996.

9.) Peracchio, A.A., Proscia, W.M., ASME paper # 98-GT-269.

10.) Lieuwen, T., Neumeier, Y., Zinn, B. T., *Comb. Sci. Tech.* V. 135, 1-6, (1998).

11.) Lieuwen, T., Zinn, B. T., AIAA paper # 98-0641 (1998).

12.) Lieuwen, T., Zinn, B.T., *Twenty Seventh Symposium (International) on Combustion*, The Combustion Institute, Pittsburgh, PA, (1998).

13.) Keller, J.J., *AIAA Journal*, Vol. 33 (12), (1995), pp. 2280-2287.

14.) Mongia, R., Dibble, R., Lovett, J., ASME Paper # 98-GT-304, (1998).

15.) Sattinger, S.S., Neumeier, Y., Nabi, A., Zinn, B.T., Amos, D.J., Darling, D.D., ASME paper # 98-GT-258 (1998).

16.) Straub, D., Richards, G., Yip, M.J., AIAA paper # 98-3909, (1998).

17.) Torres, H., Lieuwen, T., Johnson, C., Daniel, B.R., Zinn, B.T., AIAA paper # 99-0712 (1999).

18.) Putnam, A.A., *Combustion Driven Oscillations in Industry*, American Elsevier Publ. Co.: NY, 1971.

19.) Seo, S., Broda, J.C. and Santoro, R. J. personal communication (1998).

20.) Steele, Rob, *1998 AGTSR Combustion Workshop*, Berkeley, CA, Mar. 25-27, (1998).

21.) Fleifel, M., Annaswamy, A.M., Ghoniem, Z.A., Ghoniem, A.F., *Comb. and Flame*, 106: 487-510, (1996).

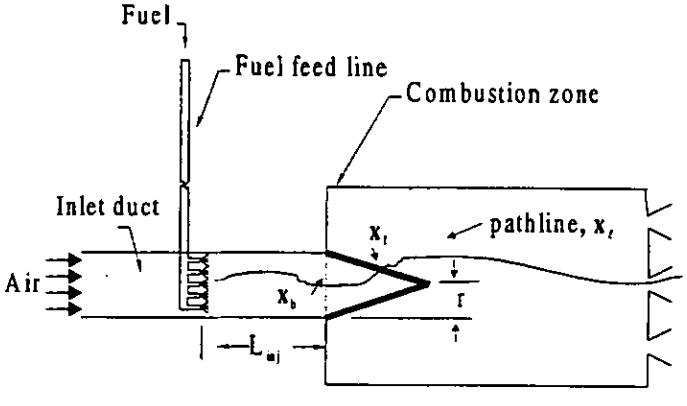

Figure 1 – A schematic of a typical LP combustor.

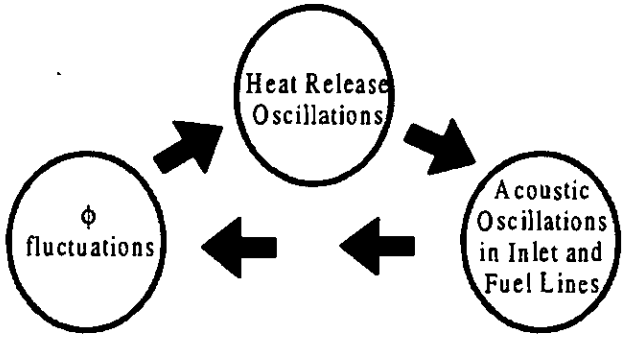

Figure 2 – A schematic of the feedback loop possibly responsible for LP combustion instabilities.

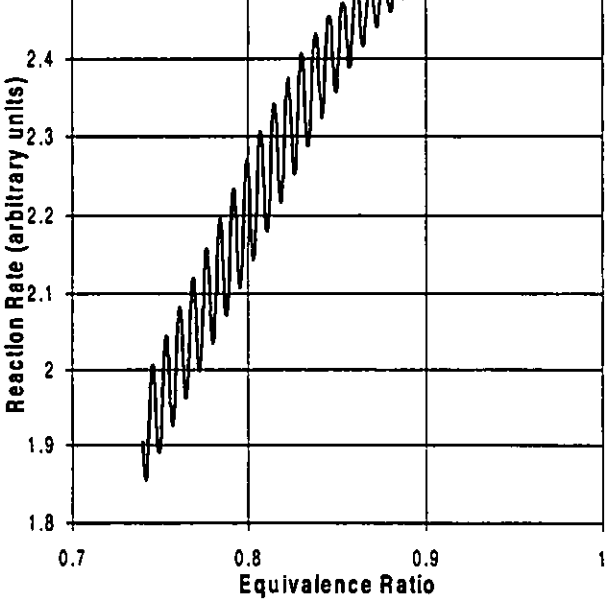

Figure 3 – Dependence of the response of the WSR reaction rate to ϕ perturbations in its inlet flow upon the mean value of ϕ.

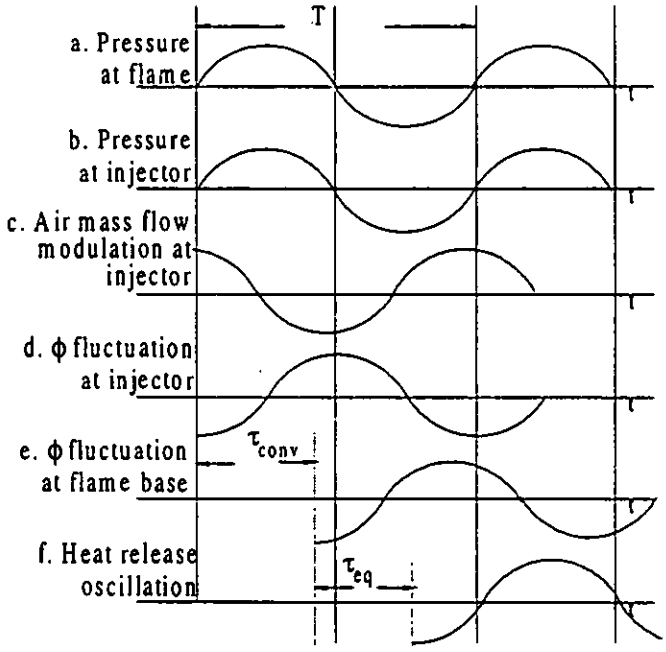

Figure 4 – A schematic showing the time evolution of disturbances responsible for a combustion instability.

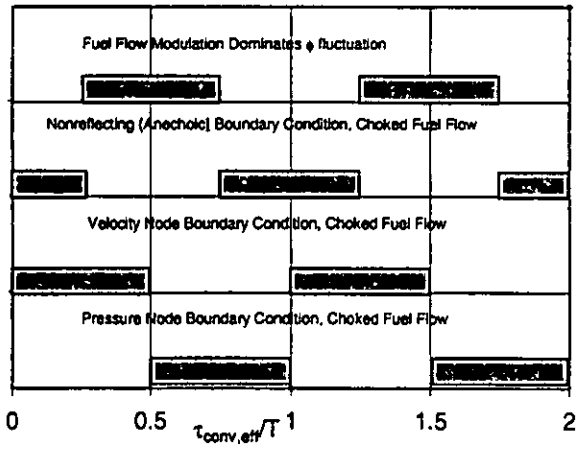


- Instability regions

Figure 5 – Dependence of instability regions upon $\tau_{conv,eff}/T$ for several different combustor configurations

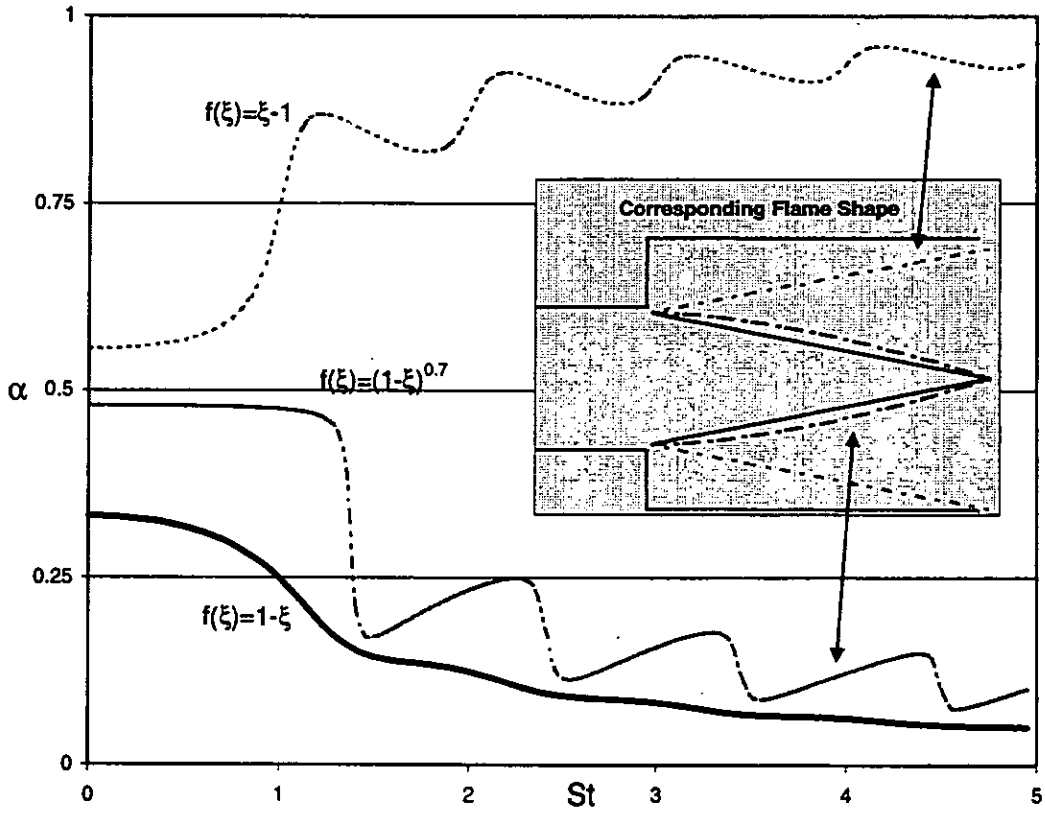

Figure 6 – Dependence of α on the flame Strouhal number, $St=fL_{flame}/u$ for three different flame shapes.

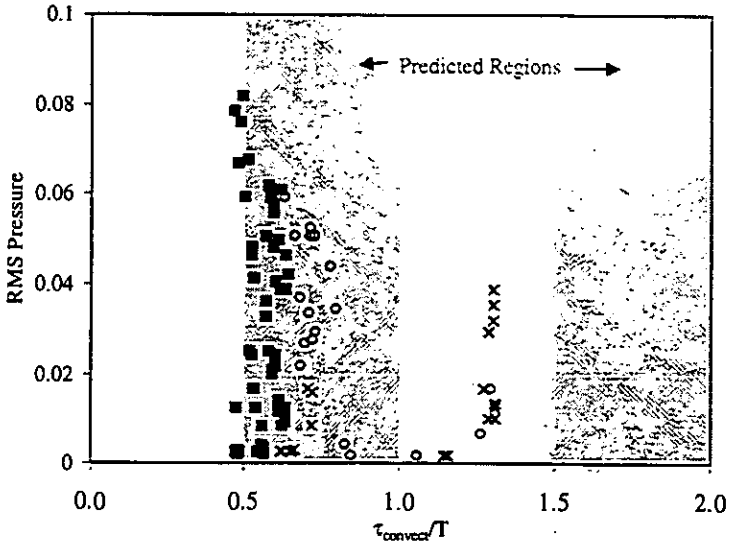

Figure 7 – Dependence of unsteady pressure amplitudes measured in a DOE combustor [3] and its predicted linear stability limits upon $\tau_{convect}/T$.

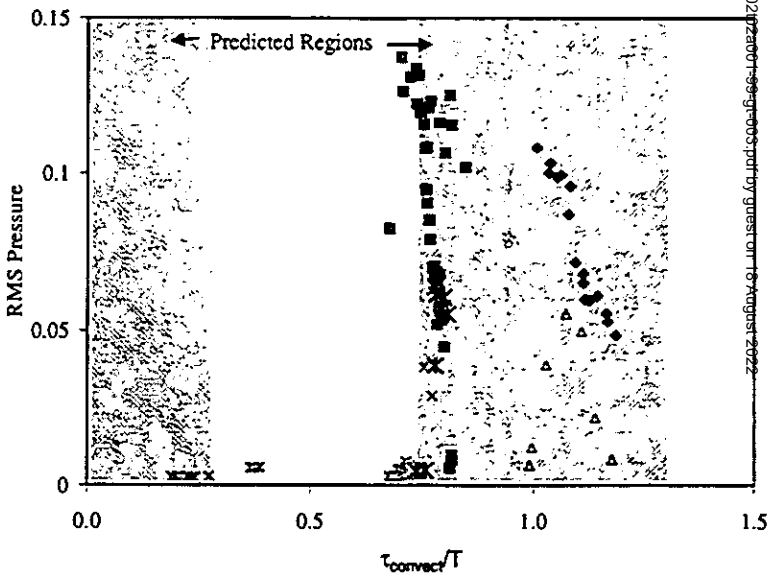

Figure 8 – Dependence of unsteady pressure amplitudes measured in a Penn State combustor [2] and its predicted linear stability limits upon $\tau_{convect}/T$.

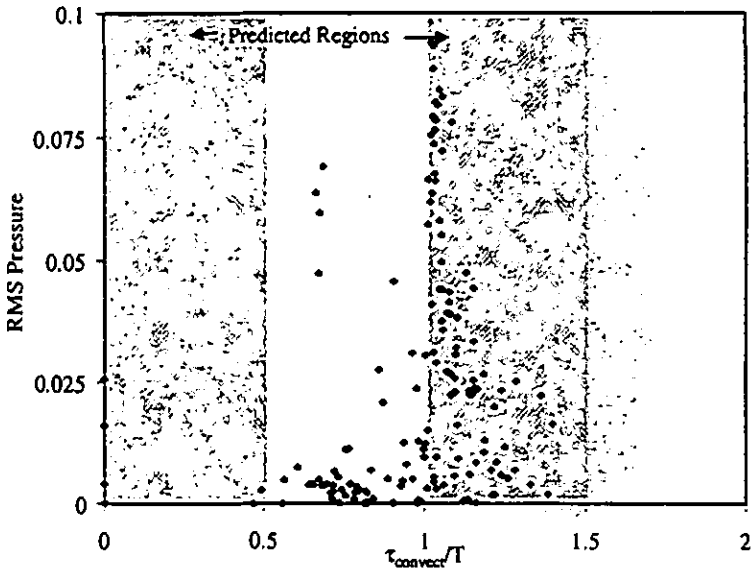

Figure 9 – Dependence of unsteady pressure amplitudes measured in a Georgia Tech combustor and its predicted linear stability limits upon $\tau_{convect}/T$.

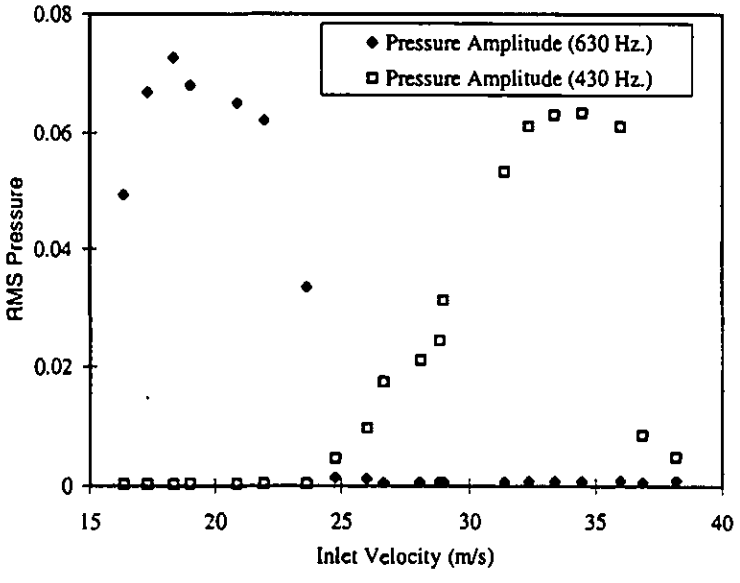

Figure 10 – Dependence of the pressure amplitudes of the 430 and 630 Hz modes, measured at Georgia Tech, upon the mean inlet velocity.